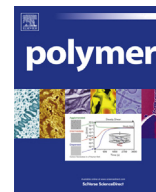




Contents lists available at SciVerse ScienceDirect

Polymer

journal homepage: www.elsevier.com/locate/polymer

The rational design of polyurea & polyurethane dielectric materials

R.G. Lorenzini^a, W.M. Kline^b, C.C. Wang^b, R. Ramprasad^b, G.A. Sotzing^{a,c,*}

^a Department of Chemistry & The Polymer Program, University of Connecticut, 97 North Eagleville Road, Storrs, CT 06268, United States

^b Department of Materials Science & Engineering, University of Connecticut, 97 North Eagleville Road, Storrs, CT 06268, United States

^c Department of Physics, University of Connecticut, 97 North Eagleville Road, Storrs, CT 06268, United States

ARTICLE INFO

Article history:

Received 18 January 2013

Received in revised form

28 April 2013

Accepted 1 May 2013

Available online xxx

Keywords:

Polymer dielectrics

Dielectric spectroscopy

Capacitors

ABSTRACT

When designing polymeric capacitors, it is important to understand the structure–property relationship between chemical functionalities and dielectric properties to tailor materials for specific applications in terms of dielectric constant, dielectric loss, band gap, breakdown strength, etc. Herein, we report a clear structure–property relationship with dielectric constant and dielectric loss in a series of polyurea and polyurethane thin films. We demonstrate that the dielectric constant systematically increases and the dielectric loss decreases as the number of carbons between polarizable functional groups decreases. Our syntheses are guided with data obtained from high-throughput density functional theory calculations. By modeling 382 polymer systems, we have determined that a dielectric constant >4 is achieved with at least one aromatic group and at least one of the following moieties: $-\text{NH}-$, $-\text{C}(=\text{O})-$, or $-\text{O}-$.

© 2013 Elsevier Ltd. All rights reserved.

1. Introduction

The development of high energy density capacitors is driven by their importance in various applications, including hybrid electric vehicles, the electric propulsion of ships [1] and electromagnetic railguns [2]. In terms of polymeric materials, biaxially oriented polypropylene (BOPP) is the current industrial standard. BOPP boasts a remarkably high electrical breakdown strength and large band gap, in addition to its ease of processability, high breakdown field and graceful failure [3]. BOPP has a dielectric constant at room temperature of ~ 2.2 across a broad frequency range and a dielectric loss in the neighborhood of 10^{-3} – 10^{-4} [4]. To add to the existing body of work in this field [5–8], we aim to understand the structure–property relationship between chemical functionalities and dielectric properties, through the paradigm of rational capacitor design. Ultimately, this level of understanding should allow for the tailoring of materials for specific electronic applications.

In the present study, we consider a large number of polymer systems with different functionalities, with the intent of identifying new polymer dielectric materials that have better dielectric properties than BOPP without sacrificing its already remarkable insulating properties. In an attempt to identify promising polymer subclasses we use first principles computations based on density

functional theory (DFT) to perform an initial combinatorial screening. This initial screening has helped us to identify organic building blocks such as aromatic rings, $-\text{NH}-$, $-\text{CO}-$, $-\text{O}-$, etc., (i.e., those that make up ureas and urethanes) as promising ones. Polymers containing these functionalities are synthesized and their dielectric properties are characterized and compared with the DFT results.

2. Computational guidance

As a first step, we used DFT computations in a high-throughput mode to identify promising cases that may lead to a high dielectric constant and high band gap; we note that the former property leads to a larger energy density, and the latter is an indicator of a good insulator (and high breakdown strength). Fig. 1 captures the computational model adopted in our strategy. In essence, we consider an all-trans single polymer chain containing four independent blocks with periodic boundary conditions along the chain axis. We allow each block in the polymer backbone to be one of following units: $-\text{CH}_2-$, $-\text{NH}-$, $-\text{C}(=\text{O})-$, $-\text{C}_6\text{H}_4-$ (benzene), $-\text{C}_4\text{H}_2\text{S}-$ (thiophene), $-\text{C}(=\text{S})-$, and $-\text{O}-$. Different combinations of these units form traditional polymers, including polyesters, polyamides, polyethers, polyureas, etc. This scheme results in 382 symmetry unique systems.

Density functional theory (DFT), as implemented in the Vienna ab initio simulation package (VASP) [9] was used to determine the structural and electronic properties of the 382 polymer chains. The Perdew, Burke, and Ernzerhof functional (PBE) [10,11], projector-

* Corresponding author. Department of Physics, University of Connecticut, 97 North Eagleville Road, Storrs, CT 06268, United States.

E-mail address: g.sotzing@uconn.edu (G.A. Sotzing).

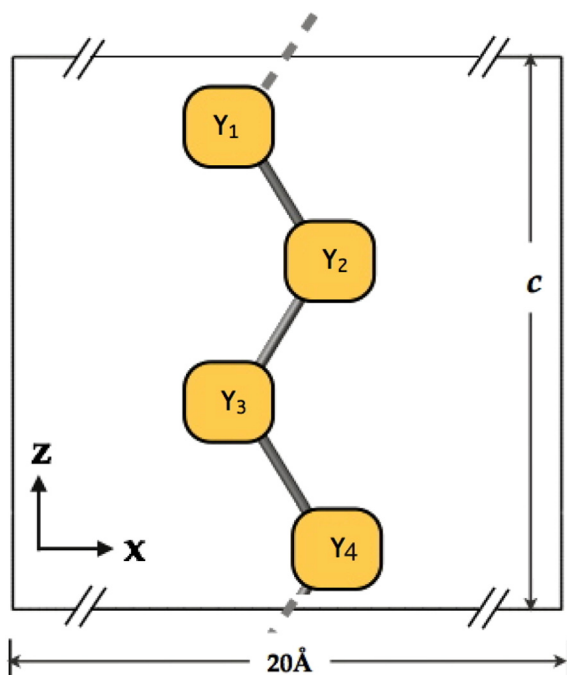


Fig. 1. Model showing our computational strategy, in which we substitute different functionalities into the four blocks. These calculations operate at the atomic scale, and therefore neglect interchain interactions.

augmented wave (PAW) frozen-core potentials [12] and a cutoff energy of 400 eV for the plane wave expansion of the wavefunctions were used. The optimized geometry was then used to determine the electronic (high frequency, or optical) and total (low frequency, or static) dielectric constant tensor of the polymer chains density functional perturbation theory (DFPT) [13], followed by extrapolation of these results to correspond to the volume actually occupied in real polymeric systems using methods developed recently [14,15].

Fig. 2 shows the relationship between the electronic (Fig. 2(a)) and total (Fig. 2(b)) dielectric constant and the band gap for the 382 polymer systems. A near perfect inverse pareto-optimal front relationship between the band gap and the electronic dielectric constant can be seen from Fig. 2(a), which imposes a theoretical limit on the electronic part of the dielectric constant that one may

be able to achieve (a limit that may be understood by regarding the electronic part of the dielectric response as a sum over electronic transitions from occupied to unoccupied states). Fig. 2(b) shows the variation of the total dielectric constant with the band gap. The total dielectric constant derives its contributions from the electronic and ionic contributions. The latter is, in principle, not constrained by the band gap, and is related to the dipole moment values of the functional groups and the flexibility of bonds that can allow the dipoles to respond to an electric field. From Fig. 2(b), a set of the most promising polymers may be selected based on the criteria that the band gap >3 eV, and total dielectric constant >4 . This “promising” region is shown in Fig. 2(b), and corresponds to systems composed of at least one aromatic group and at least one of the following three groups: $-\text{NH}-$, $-\text{C}(=\text{O})-$, $-\text{O}-$.

The DFT-recommended groups provided useful constraints for determining the best functionalities to incorporate into a polymer backbone. We understood that polymers synthesized for electronic applications should be as pure as possible; we sought to eliminate impurities that were both catalytic and inherent in nature. To this end, we ultimately decided on polyureas and polyurethanes derived from the step polymerization of an asymmetrically substituted aromatic diisocyanate and various diols and diamines (Fig. 3) – these systems were harmonious with the results of the DFT calculations, produced no byproducts, and required little or no catalyst.

3. Polymer synthesis

3.1. Materials

Reagents and solvent were purchased from Acros Organics or Sigma–Aldrich, with the exception of the 2,2′-oxybis-ethanamine, which was purchased from Huntsman. Liquids were purified either by ambient pressure distillation or vacuum distillation and were stored under nitrogen.

3.2. Polyurea and polyurethane syntheses

To a nitrogen-filled, flame-dried 25 mL 3-neck flask equipped with a gas inlet, rubber and glass stoppers and a magnetic stirbar, 10 mL of dimethylsulfoxide was added via cannula needle. Next, 5 mmol of diamine/diol was cannulated; the materials used were: 1,2-diaminoethane, 1,2-diaminopropane, 1,3-diaminopropane, 1,6-diaminohexane, 2,2′-oxybis-ethanamine, 1,2-ethanediol, 1,2-

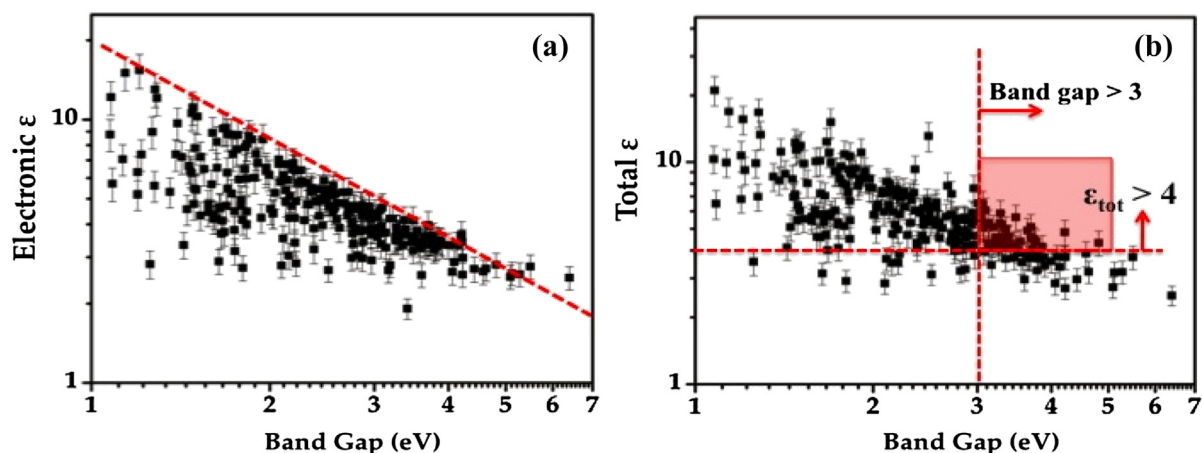


Fig. 2. DFT computed (a) electronic and (b) total dielectric constant along the polymer chain axis as a function of the band gap. The axes are in logarithmic scale.

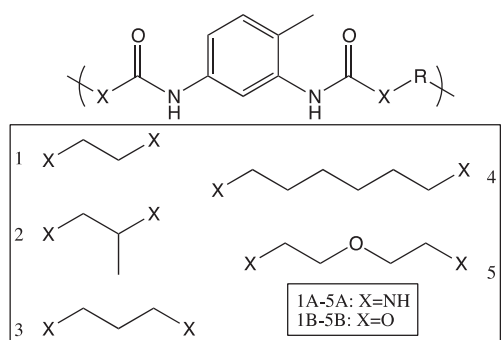


Fig. 3. Structures of synthesized polyureas and polyurethanes.

propanediol, 1,3-propanediol, 1,6-hexanediol, diethylene glycol. In the case of the diols, 1 wt% of dibutyltin dilaurate was added as a catalyst. Cannulation of 5 mmol of 2,4-toluene diisocyanate (TDI) initiated an exothermic event. When the temperature from the initial mixing subsided, an oil bath was used to heat the mixture to 60 °C for 2 h. The resultant polymers were precipitated in methanol, and were allowed to stir in the methanol for 1 h to remove any excess monomer/catalyst, after which they were filtered using a Büchner funnel and dried *in vacuo* for 24 h at 160 °C. This cleaning and heating protocol ensured complete removal of solvent, excess monomer and methanol-soluble oligomers, as confirmed by a GC/MS polymer desorption method. In all cases, the polymers were obtained in nearly quantitative yields.

3.3. Film preparation for TDDS

Polymer samples were prepared for films as follows: 5 wt% solutions of polymer/DMSO were prepared by heating, stirring and filtration through a 0.45 μm PTFE syringe filter. Polymer films were drop cast on stainless steel shims, and were left on the bench overnight to allow a bit of solvent to evaporate off, leaving a “tacky” film. These tacky samples were then heated in a vacuum oven for 160 °C overnight to ensure complete removal of solvent. During all steps, care was taken to prevent the introduction of dust from the laboratory, such as the use of petri dishes for solvent evaporation. Polymer films prepared in this way were determined to be 200–400 nm thick.

Table 1

The dielectric constant and dielectric loss of the polyureas at 60 Hz and 1 kHz at various temperatures.

Polyureas						
Polymer	Room temp.		50 °C		100 °C	
	ϵ	ϵ	ϵ	ϵ	ϵ	ϵ
	60 Hz	1 kHz	60 Hz	1 kHz	60 Hz	1 kHz
1A	5.24	5.18	5.31	5.23	6.63	5.85
2A	4.35	4.29	4.50	4.38	5.92	5.13
3A	3.54	3.47	3.55	3.48	3.45	3.38
4A	2.17	2.08	2.23	2.13	2.20	2.11
5A	6.72	6.19	7.03	6.44	7.22	6.87

Polymer	$\tan(\delta)$		$\tan(\delta)$		$\tan(\delta)$	
	$\tan(\delta)$	$\tan(\delta)$	$\tan(\delta)$	$\tan(\delta)$	$\tan(\delta)$	$\tan(\delta)$
	60 Hz	1 kHz	60 Hz	1 kHz	60 Hz	1 kHz
1A	0.00683	0.00758	0.00883	0.00862	0.116	0.0539
2A	0.00941	0.00889	0.0179	0.0135	0.116	0.0675
3A	0.0117	0.0173	0.0130	0.0176	0.0141	0.0124
4A	0.0222	0.0312	0.0259	0.0323	0.0261	0.0242
5A	0.0342	0.0429	0.0322	0.0543	0.0266	0.0444

Table 2

The dielectric constant and dielectric loss of the polyurethanes at 60 Hz and 1 kHz at various temperatures.

Polyurethanes						
Polymer	Room temp.		50 °C		100 °C	
	ϵ	ϵ	ϵ	ϵ	ϵ	ϵ
	60 Hz	1 kHz	60 Hz	1 kHz	60 Hz	1 kHz
1B	6.47	6.35	6.71	6.52	9.75	8.43
2B	6.87	6.74	6.84	6.73	6.90	6.74
3B	5.96	5.81	4.72	4.54	6.37	5.63
4B	4.22	4.09	4.29	4.15	4.52	4.37
5B	10.8	10.5	11.0	10.6	13.8	12.0

Polymer	$\tan(\delta)$		$\tan(\delta)$		$\tan(\delta)$	
	$\tan(\delta)$	$\tan(\delta)$	$\tan(\delta)$	$\tan(\delta)$	$\tan(\delta)$	$\tan(\delta)$
	60 Hz	1 kHz	60 Hz	1 kHz	60 Hz	1 kHz
1B	0.0113	0.0126	0.0178	0.0157	0.1190	0.0650
2B	0.00896	0.0154	0.00874	0.0136	0.0138	0.0140
3B	0.0158	0.0139	0.0211	0.0210	0.0980	0.0608
4B	0.0184	0.0156	0.0167	0.0180	0.0220	0.0220
5B	0.0151	0.0188	0.0168	0.0201	0.135	0.0615

3.4. TDDS spectroscopy

The dielectric spectra were obtained on an IMASS time domain dielectric spectrometer at the University of Connecticut Electrical Insulation Research Center. Measurements were taken at room temperature, 50 °C and 100 °C between silicone rubber guarded electrodes.

3.5. Polymer characterization

^1H NMR data was obtained on a Bruker DMX-500, and IR spectroscopy was performed on a Nicolet Magna-IR 560 spectrometer. Thermogravimetric analysis was conducted on a TA

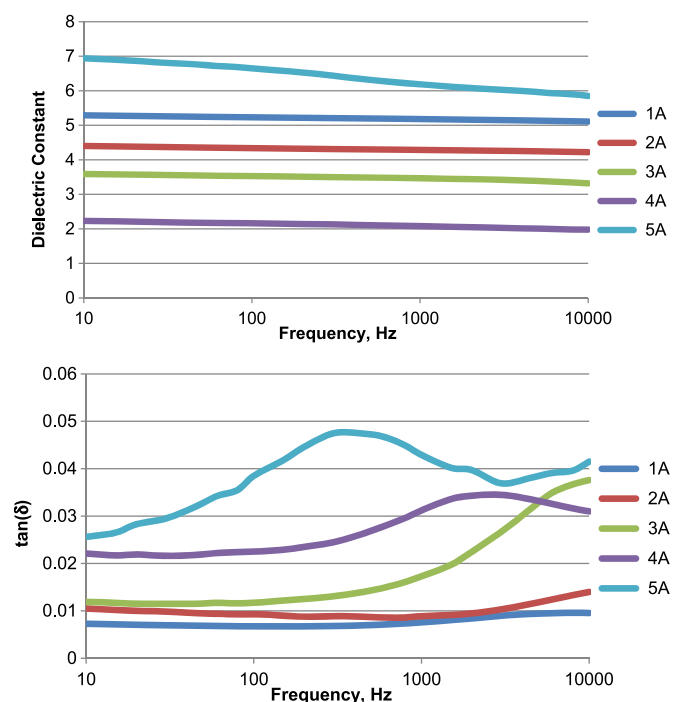


Fig. 4. Dielectric constant (top) and $\tan(\delta)$ (bottom) at room temperature for the different polyureas.

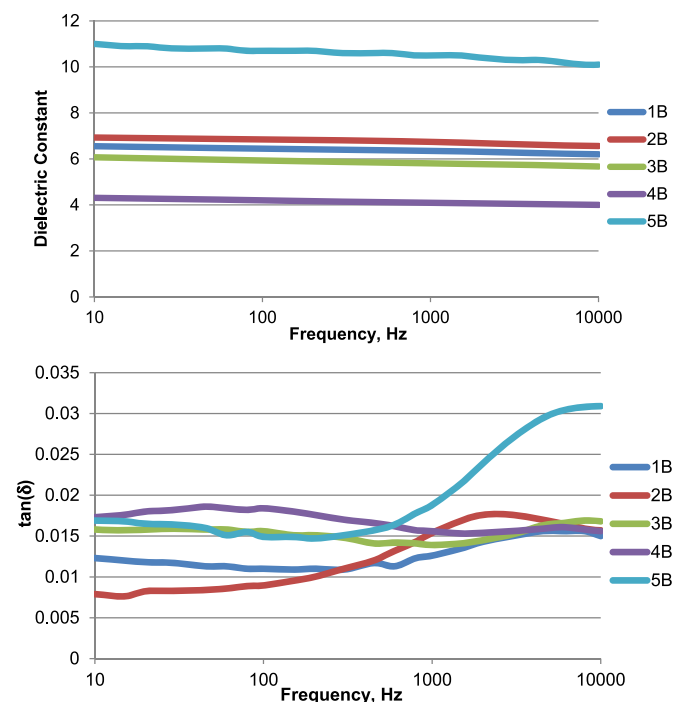


Fig. 5. Dielectric constant (top) and $\tan(\delta)$ (bottom) at room temperature for the different polyurethanes.

Instruments TGA Q500 by heating 10 °C/min from room temperature to 500 °C in oxygen; the data presented represents the temperature at 3% weight loss. Differential scanning calorimetry was performed on a TA Instruments DSC Q100: first, the sample was heated at 10 °C/min to just before its weight loss onset temperature, and was held isothermally for 5 min. It was then cooled to –50 °C at 10 °C/min. Data was obtained on the next cycle, when the sample was heated to the 3% degradation temperature at 10 °C/min. Gel permeation chromatography was conducted using dimethylacetamide as the mobile phase and polystyrene standards with the following instrumentation: Waters 515 HPLC pump, Waters 2414 refractive index detector, two mixed bed Jordi Gel DVB columns. Samples were filtered twice prior to GPC analysis: first with a Kimwipe-plugged pipette to remove large insoluble materials, and second with a 0.45 μm PTFE syringe filter.

Table 3

Table containing the glass transition temperature (T_g), melting temperature (T_m) and 3% degradation temperature (T_d) for each of the sample polymers. All temperatures are reported in °C.

Polymer	T_g	T_m	T_d
<i>Polyureas</i>			
1A	N/O	242	246
2A	N/O	228	234
3A	N/O	234	227
4A	N/O	224	263
5A	N/O	201	264
<i>Polyurethanes</i>			
1B	130	N/O	237
2B	75	N/O	251
3B	72	215	251
4B	95	213	277
5B	91	167	249

Table 4

Table containing the number-average molecular weight (M_n), the weight-average molecular weight (M_w), and the polydispersity index (PDI). All molecular weights are reported in g/mol.

Polymer	M_n	M_w	PDI
<i>Polyureas</i>			
1A	Not soluble		
2A	Not soluble		
3A	37,500	54,400	1.45
4A	31,400	41,200	1.31
5A	29,100	39,500	1.36
<i>Polyurethanes</i>			
1B	24,300	37,800	1.56
2B	19,600	28,900	1.47
3B	28,700	36,400	1.27
4B	21,700	30,800	1.42
5B	37,900	49,400	1.30

4. Results & discussion

4.1. TDDS spectroscopy results

For all of the polymers, the dielectric constant and dielectric loss at 60 Hz and 1 kHz are tabulated (Tables 1 and 2). In addition, the room temperature dielectric spectra are overlaid (Figs. 4 and 5).

4.2. Structure–property relationship: polymer classes, alkyl length, dielectric constant & loss

The dielectric behavior of these materials can be explained through several paradigms. Most generally, polyurethanes have higher dielectric constants than polyureas, which is reasonable based on electronegativity arguments. These data suggest that for both classes of polymers, increasing the number of carbons in the backbone lowers the dielectric constant. This can be attributed to the increase in free volume, which decreases the number of polarizable groups per unit volume [16,17]. Inclusion of a backbone ether moiety (5a&b) drastically increases the dielectric constant in both cases, in agreement with literature values for polyether polyurethanes; more ether oxygen atoms present in the backbone result in higher dielectric constants [18]. The dielectric loss $\tan(\delta)$ is also observed to follow the aforementioned trend: smaller alkyl spacers yield lower loss values. These conclusions are in agreement with generally accepted means of increasing dielectric constant, including maximizing polarizability and imparting a low degree of free volume [19].

4.3. Polymer characterization

Due to the structural similarity of the polymers being tested, differences in the NMR and IR spectra were difficult to discern. However, we used these data to both confirm the purity of the materials and the absence of reactive isocyanate end groups, which would manifest themselves in the IR as a sharp peak at $\sim 2250 \text{ cm}^{-1}$. The TGA (3% degradation) and DSC data are presented below (Table 3), demonstrating high thermal stability well beyond the operating temperature of BOPP. The low polydispersity (Table 4) observed in these polymers likely has to do with the workup conditions – stirring in methanol removed some of the lower weight chains. A study comparing the dielectric constants and losses of polypropylene glycols with varying molecular weights shows that the dielectric properties saturate between 1000 and 2000 g/mol [20].

5. Conclusions & summary

This study was primarily intended to span the chemical space, searching for the paramount influences of structure on dielectric

constant. Our synthetic efforts were guided by DFT calculations, which revealed that polymers with high dielectric constants contain at least one aromatic group, and one of three functionalities: $-\text{NH}-$, $-\text{C}(=\text{O})-$, or $-\text{O}-$; the majority of the synthesized polymers had dielectric constants >4 as predicted by said calculations. These dielectric data will be conglomerated with data from parallel synthetic efforts in our group, to be fed into a quantitative structure–activity relationship model (QSAR) to be published at a later date. Our ultimate aim is to investigate materials with more desirable electronic properties (higher dielectric constant, higher band gap, comparable loss) compared with the current industry standard BOPP, and we consider this work to be generally successful toward our goal. Most of the aforementioned materials can operate at or beyond BOPP's failure temperature, which successfully operates between 60 and 80 °C [21]. BOPP has a dielectric constant of 2.2; the dielectric constants reported herein are either equal to or higher than BOPP. BOPP has loss values in the 10^{-3} – 10^{-4} regime, whereas our lowest loss polymer (1A) is towards the upper end of this range ($6.8 * 10^{-3}$).

Acknowledgments

We would like to thank Ms. JoAnne Ronzello and Dr. Steven A. Boggs of the University of Connecticut Electrical Insulation Research Center for dielectric testing and helpful suggestions. In addition, we would like to express gratitude for financial support from the Office of Naval Research through the Multidisciplinary University Research Initiative (MURI).

References

- [1] Flynn PF. Meeting the energy needs of future warriors. Washington D.C.: National Academics Press; 2004.
- [2] Electromagnetic railgun. Office of naval research fact sheet. <http://www.onr.navy.mil/Media-Center/Fact-Sheets/Electromagnetic-Railgun.aspx>; Feb. 2012.
- [3] Sarjeant WJ, Zirnheld J. Handbook of low and high dielectric constant materials and their applications. UK: Academic Press; 1999.
- [4] Ho J, Jow R. Characterization of high temperature polymer thin films for power conditioning capacitors. Army Research Laboratories; Jul. 2009. ARL-TR-4880.
- [5] Zhang Q, Zhu D, Su F, Xie Y, Ma Z, Shen J. J Biomed Mater Res A 2012;100A(7): 1868–76.
- [6] Wang Y, Zhou X, Chen Q, Chu B, Zhang QM. IEEE Trans Dielectr Electr Insul 2010;17(4):1036–42.
- [7] Oprea S, Potolinca O, Oprea V. High Perform Polym 2011;23(1):49–58.
- [8] Adjokatse SK, Mishra AK, Waghmare UV. Polymer 2012;53:2751–7.
- [9] Kresse G, Furthmuller J. Phys Rev B 1996;54:11169.
- [10] Perdew JP, Burke K, Ernzerhof M. Phys Rev Lett 1996;77:3865.
- [11] Blochl PE. Phys Rev B 1994;50:17953.
- [12] Kresse G, Joubert D. Phys Rev B 1999;59:1758.
- [13] Baroni S, de Gironcoli Stefano, Dal Corso Andrea. Rev Mod Phys 2001;73: 515.
- [14] Pilania G, Ramprasad R. J Mater Sci 2012;47:7580.
- [15] Wang CC, Pilania G, Ramprasad R. Submitted for publication.
- [16] Simpson JO, St.Clair AK. Fundamental insight on developing low dielectric constant polyimides. Thin Solid Films 1997;308–309:480–5.
- [17] Hwang H-J, Li C-H, Wang C-S. Polymer 2006;47:1291–9.
- [18] North AM, Reid JC. Dielectric relaxation in a series of heterophase polyether polyurethanes. Eur Polym J 1972;8:1129–38.
- [19] Deligoz H, Ozgumus S, Yalcinyuva T, Yildirim S, Deger D, Ulutas K. Polymer 2005;46:3720–9.
- [20] Sarode AV, Kumbharkhane AC. J Mol Liq 2011;160:109–13.
- [21] Zou C, Zhang Q, Zhang S, Kushner D, Zhou X, Bernard R, et al. PEN/Si₃N₄ bilayer film for DC bus capacitors in power converters in hybrid electric vehicles. J Vac Sci Technol B 2011;29:061401.